# Evaluation of Thermodynamic Properties of Solids by Quasiharmonic Lattice Dynamics[1]

**N. L. Allan,**[2] **G. D. Barrera,**[3] **T. H. K. Barron,**[2, 4] **and M. B. Taylor**[2]

Quasiharmonic lattice dynamics is a simulation technique complementary to Monte Carlo and molecular dynamics. Quantum effects are readily taken into account, and high precision does not normally require long runs. Vibrational stability is a sensitive test of interatomic potentials, and details of the vibrational motion reveal mechanisms for phase transitions or for thermal expansion. The major computational task is usually to find the equilibrium geometry at a given $T$, $P$; this done, calculating free energy, heat capacity, thermal expansion, etc., is rapid and accurate. For three-dimensional ionic crystals and slabs, our code SHELL calculates *analytically* first derivatives of the free energy with respect to all strains, internal as well as external; this gives a full minimization of the free energy so efficient that *large unit cells* can be used, allowing applications to defects and disordered systems. Various applications are discussed: $MgF_2$, including the rutile/fluorite transition; negative thermal expansion in $ZrW_2O_8$; anisotropic expansion of polyethylene at very low temperatures; surface free energies for MgO; defect energies and volumes in MgO; and a new method for obtaining free energies and phase diagrams of disordered solids and solid solutions, applied to MnO/MgO and CaO/MgO.

**KEY WORDS:** defects; free energy minimisation; lattice dynamics; low temperatures; solid solutions; thermal expansion.

## 1. INTRODUCTION

Quasiharmonic lattice dynamics (QLD) is a relatively inexpensive technique, which avoids the kinetic barriers and critical slowing-down effects

---

[2] School of Chemistry, University of Bristol, Cantock's Close, Bristol BS8 1TS, United Kingdom.

[3] Departamento de Química, Universidad Nacional de la Patagonia SJB, Ciudad Universitaria, (9000) Comodoro Rivadavia, Argentina.

[4] To whom correspondence should be addressed. E-mail: t.h.k.barron@bris.ac.uk

suffered by Monte Carlo (MC) and molecular dynamics (MD) and has the advantage that free energies and derived properties such as entropy and heat capacity can be calculated directly with a high precision. QLD also gives a sensitive test for interatomic potentials, in that imaginary phonon frequencies may indicate at once that a trial potential is invalid. The main disadvantage is that QLD is valid only when vibrational amplitudes are fairly small, and so other techniques must be used at high temperatures as melting is approached. We first outline the technique, as applied by our recent code SHELL [1], and then present the set of illustrative examples listed in the abstract.

## 2. THEORETICAL METHODS

Our new code SHELL [1] uses both lattice statics and QLD, and is designed for the efficient study of solids and slabs with periodic structures and *many* internal strains. In its present form, two- and three-body potentials represent short-range forces. Ionic and polarizability effects are taken into account by using the well-known shell model, in which each ion consists of a massive "core" and a massless "shell"; both core and shell are charged, and so their relative displacement produces an electric dipole.

For structure optimization, we minimize the free energy using its strain derivatives. Most previous work has used the *z*ero *s*tatic *i*nternal *s*tress *a*pproximation (ZSISA), or minor variations thereof, in which only external coordinates (dimensions of the unit cell) are relaxed using fully dynamic free energy derivatives, while internal coordinates (positions of the ions in the unit cell) are relaxed using static energy derivatives. The static energy derivatives are easy to calculate analytically and the small number of external free energy derivatives are obtained numerically. ZSISA gives optimized external coordinates correctly to first order [2], but to get correct internal coordinates requires a full minimization of the free energy with respect to all coordinates; and even for moderately sized unit cells, to do this by numerical differentiation is normally prohibitively expensive. SHELL therefore adopts a method suggested for complex ionic crystals by Kantorovich [3] and calculates the full set of free energy first derivatives analytically; this makes possible a valid treatment of the atomic positions within the unit cell.

For optimization at an applied pressure $P_{ext}$, we minimize the "availability" [4] $\tilde{G} = F + P_{ext} V$ with respect to all strains. In QLD the Helmholtz free energy, $F$, at temperature $T$ is the sum of static and vibrational contributions:

$$F(\mathscr{E}, T) = \Phi_{stat}(\mathscr{E}) + F_{vib}(\mathscr{E}, T) \tag{1}$$

where $\mathscr{E}$ denotes the full set of strain variables, comprising both external ($\eta_\lambda$) and internal ($\varepsilon_k$) strains. $\Phi_{\text{stat}}$ is thus the potential energy of the static lattice in a given state of strain $\mathscr{E}$. Traditional static lattice simulations evaluate only $\Phi_{\text{stat}}$ and its strain derivatives.

$F_{\text{vib}}$ is the sum of harmonic vibrational contributions from all the normal modes of vibration and, for a periodic structure, is given by

$$F_{\text{vib}} = \sum_{\mathbf{q},\, j} \left\{ \tfrac{1}{2} h v_j(\mathbf{q}) + k_{\text{B}} T \ln[\, 1 - \exp(-h v_j(\mathbf{q})/k_{\text{B}} T)\,]\right\} \qquad (2)$$

in which the first term is the zero-point energy. The frequencies $v_j(\mathbf{q})$ of modes with wavevector $\mathbf{q}$ are obtained by diagonalizing the dynamical matrix $D(\mathbf{q})$ [5], which is a function of the strain $\mathscr{E}$. The strain derivatives are given by

$$\left(\frac{\partial F_{\text{vib}}}{\partial \mathscr{E}_{\text{A}}}\right)_{\mathscr{E}',\, T} = \sum_{\mathbf{q},\, j} \left\{ \frac{h}{2 v_j(\mathbf{q})} \left(\frac{1}{2} + \frac{1}{\exp(h v_j(\mathbf{q})/k_{\text{B}} T) - 1}\right) \left(\frac{\partial v_j^2(\mathbf{q})}{\partial \mathscr{E}_{\text{A}}}\right)_{\mathscr{E}'} \right\} \qquad (3)$$

where $\mathscr{E}'$ denotes that all the $\mathscr{E}$ are kept constant except for the differentiation variable $\mathscr{E}_{\text{A}}$. SHELL uses first-order perturbation theory to derive $(\partial v_j^2(\mathbf{q})/\partial \mathscr{E}_{\text{A}})_{\mathscr{E}'}$ from analytic expressions for $(\partial D/\partial \mathscr{E}_{\text{A}})_{\mathscr{E}'}$. Details and full expressions are given in Refs. 6–8. A variable metric method [9] is used to minimize $F + P_{\text{ext}} V$ with respect to the $\mathscr{E}_{\text{A}}$. The static energy Hessian, $(\partial^2 \Phi_{\text{stat}}/\partial \mathscr{E}_{\text{A}}\, \partial \mathscr{E}_{\text{B}})$, is used as an approximation to $(\partial^2 F/\partial \mathscr{E}_{\text{A}}\, \partial \mathscr{E}_{\text{B}})$ in the first step; in subsequent iterations the $(\partial F/\partial \mathscr{E}_{\text{A}})$ are calculated in the new configuration and the inverse Hessian updated.

The reliability of QLD at high temperatures can be investigated by comparison with classical MC or MD simulations. For ionic solids we have found that QLD is usually valid up to about one-half to two-thirds of the melting point.

## 3. APPLICATIONS

### 3.1. MgF$_2$

Our simplest example is the rutile phase of $MgF_2$, which has a small unit cell with only one internal degree of freedom. The potentials are derived from a calculated Hartree–Fock (HF) potential energy hypersurface [10]. We have carried out not only QLD, but also MD and MC simulations for comparison. The latter two used a simulation cell containing 192 Mg and 384 F ions arranged initially in a box of sides $4 \times 4.52$,

$4 \times 4.52$, and $6 \times 3.09$ Å. In the MC simulations, the thermodynamic data were collected over $10^7$ steps after a $10^7$-step equilibration.

HF theory generally overestimates lattice parameters, and for $MgF_2$ the HF lattice parameters $a$ and $c$ are slightly larger than experiment [11]. For the new potential obtained by fitting to HF energies, $a$ is too small by about 0.3% and $c$ too large by about 4% (Fig. 1). However, the variation with $T$ of $a$ and $c$ is close to experiment. *Below* the Debye temperature $(\Theta_D)$ the MC values for $a$ and $c$ are slightly lower than the QLD values, because only QLD takes account of quantum effects (largely zero-point vibration) which expand the lattice by a small amount. The MC and MD results are in good agreement. Around $\Theta_D$ the QLD results are in good agreement with MC and MD, but for $T \geqslant 1300$ K they diverge, a characteristic indication that the quasiharmonic approximation is starting to fail.

Simulations are a valuable means of examining widely used quantities for which data are sparse. For example, one key quantity in geophysics is the isothermal Anderson–Grüneisen function, $\delta_T$, and its variation with pressure,

$$\delta_T = -(\partial \ln B_{\mathscr{T}}/\partial \ln V)_P = -(\partial \ln \beta/\partial \ln V)_T \qquad (4)$$

where $\beta$ is the volumetric thermal expansion coefficient $[ = (\partial V/\partial T)_P/V]$ and $B_{\mathscr{T}}$ the isothermal bulk modulus. For the rutile phase of $MgF_2$ over its entire pressure range, we find that $\beta$ is approximately proportional to $V^t$ at 300 K, where $t \approx 7$, so giving $\delta_T$ a constant value of 7. For the fluorite phase adopted at high pressures [10], in contrast, $\delta_T$ decreases with pressure, from $\approx 5.7$ at the transition to $\approx 4.7$ at 80 GPa.

## 3.2. Negative Thermal Expansion—$ZrW_2O_8$

$ZrW_2O_8$ exhibits large *negative* thermal expansion [12, 13] from 0.3 to 1050 K; at 428 K there is a transition to a disordered phase, but the ordered phase provides an excellent test of our methods. The unit cell is cubic and comprised of $WO_4$ tetrahedra sharing corners and $ZrO_6$ octahedra linked in such a way that each octahedron shares corners with six different $WO_4$ tetrahedra. Each $WO_4$ tetrahedron shares only three of its four oxygens with adjacent $ZrO_6$ octahedra.

Our QLD calculations for $ZrW_2O_8$ are analogous to those for $MgF_2$. For the intraoctahedron O–Zr–O and intratetrahedron O–W–O interactions, we used a Urey-energy term, $E = \frac{1}{2}k(r_{O-O} - r_e)^2$, where $r_{O-O}$ is the O–O distance and $r_e$ a constant, rather than an angle term. The calculated linear thermal expansion coefficient $\alpha$ $(= \beta/3)$ over the range 50 to 300 K is $-3.5 \times 10^{-6}$ K$^{-1}$ (experiment $\approx -8.3 \times 10^{-6}$ K$^{-1}$ [13]).
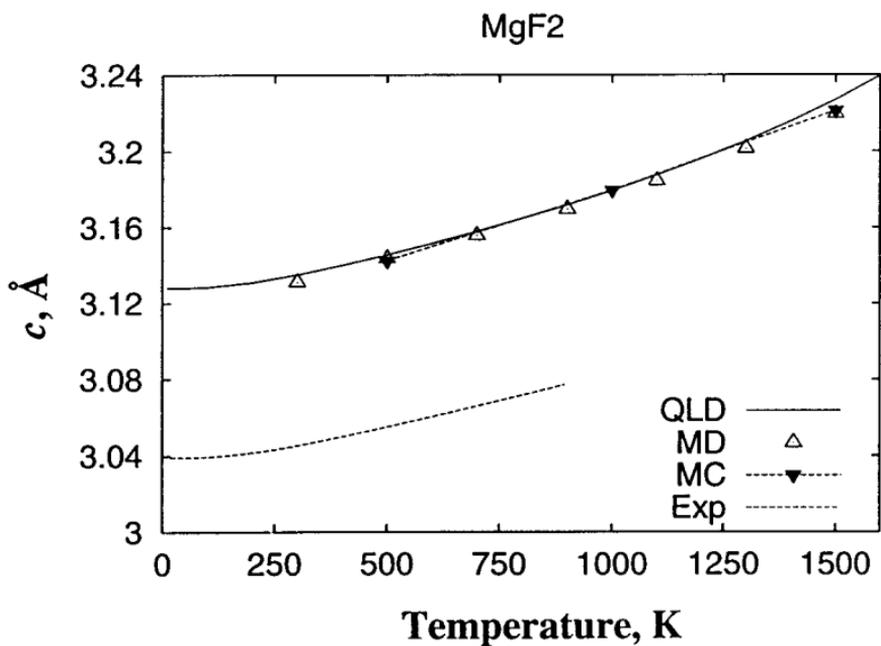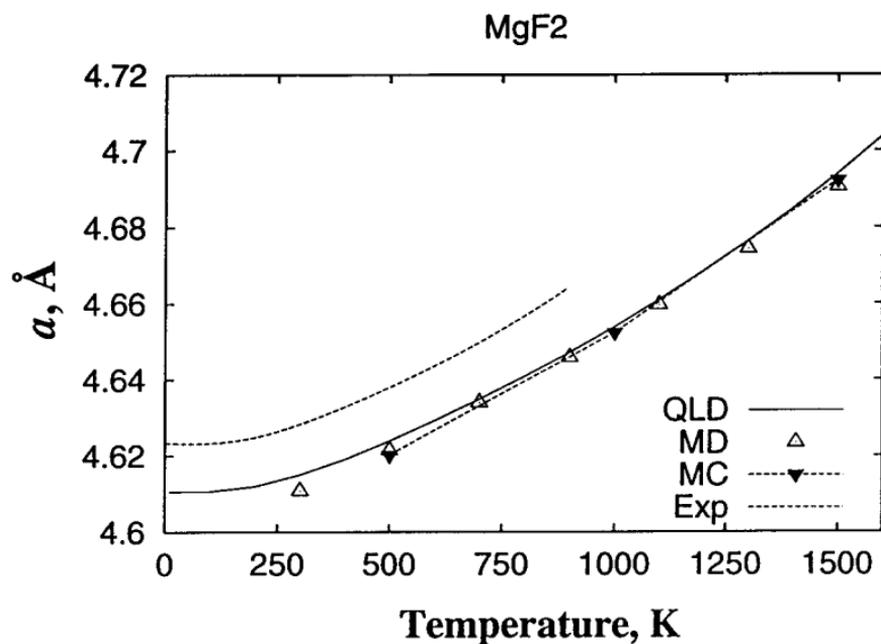
**Fig. 1.** Calculated values of *a* and *c* for $MgF_2$, with experimental data from Ref. 11.

To understand why this type of cubic structure has negative thermal expansion, we recall the thermodynamic relation $\beta = (\partial S/\partial V)_T/B_{\mathscr{T}}$. Since $B_{\mathscr{T}}$ is always positive, $\beta$ and $(\partial S/\partial V)_T$ have the same sign. $(\partial S/\partial V)_T$ is negative for $ZrW_2O_8$, due largely to the Zr–O–W transverse vibrations, which increase in frequency with increasing Zr–W internuclear separation (cf. the transverse vibrations of a stretched violin string). This *tension effect* [14] predominates, in general, only in open structures. A useful and related treatment in terms of "rigid unit modes" has been given by Pryde et al. [15].

At pressures over 0.2 GPa, cubic $ZrW_2O_8$ undergoes a phase transition to a denser orthorhombic phase [16]. In this less open structure, both calculated and observed expansion coefficients are negative and an order of magnitude smaller than for the cubic phase.

## 3.3. Very Low Temperatures—Polyethylene

At low temperatures, $C_P$ and expansion coefficients $\alpha_\lambda$ are very small, tending to zero as $T \to 0$; but they can be measured down to $\approx 1$ K or lower by sensitive techniques [17, 18]. Such measurements give information about low energy levels and their strain dependence. At these temperatures MC and MD cannot simulate $C_P$ and $\alpha_\lambda$, but the analytical methods of QLD obtain them to a high precision if increasingly fine grids are used for integrating over $\mathbf{q}$ as $\mathbf{q} = 0$ is approached [19].

We have applied QLD to short-range models of orthorhombic polyethylene [20]. The unit cell has 3 external and 6 internal degrees of freedom. Zigzag polymer chains run in the $c$-direction, interacting weakly with neighboring chains, so that $c_{33}$ is much larger than $c_{11}$ or $c_{22}$; $\alpha_c$ is therefore small and negative because of the tension effect in the C–C bonds. Above 100 K, X-ray diffraction shows that $\alpha_a$ and $\alpha_b$ are positive, with $\alpha_a$ about double $\alpha_b$. At low temperatures dilatometric measurements on drawn samples show that the mean of $\alpha_a$ and $\alpha_b$ remains positive but do not give separate values. All our models indicate that below about 10 K the anisotropy between $\alpha_a$ and $\alpha_b$ is greatly reduced or even reversed, due largely to a "rotational tension" effect [14] that rotates bonds in crystals of low symmetry.

## 3.4. Surface Free Energies

We have used full minimization of the free energy to study the $\{001\}$ and $\{110\}$ surfaces of MgO, using a well-established set of shell-model potentials [21]. Our strategy differs from the two-region strategy commonly used for static calculations [22, 23]. We consider a slab, infinite in
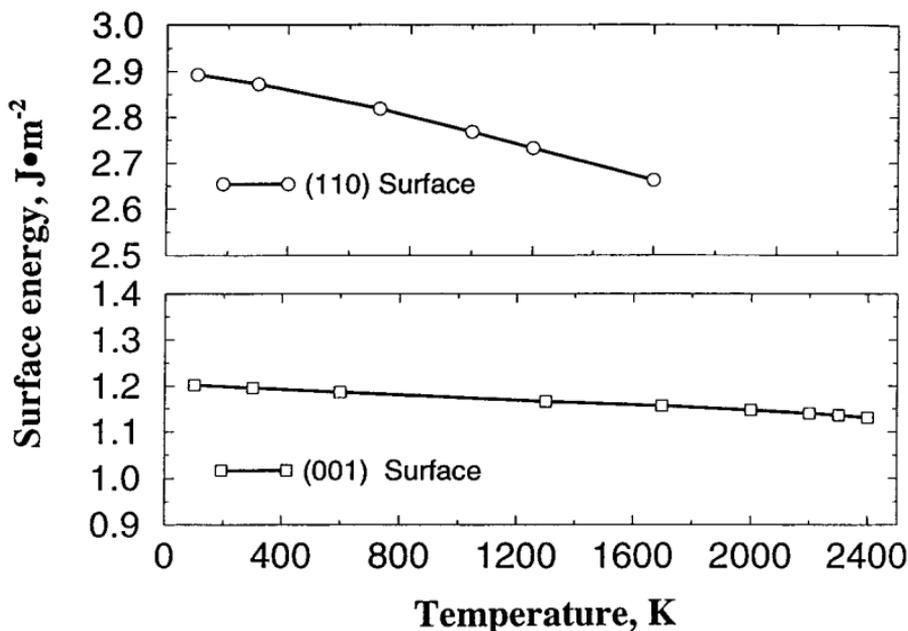
**Fig. 2.** Calculated surface energies for MgO.

two directions and finite in the other. For a thick enough slab the two faces are essentially noninteracting and can be taken as free surfaces.

Figure 2 shows the calculated temperature dependence of the surface energies. About 10 layers give convergence to 0.001 $J \cdot m^{-2}$, more than twice the number of layers needed for the static energy to converge. Both surface energies decrease with temperature, the {110} rather more markedly. Imaginary frequencies appear at $\approx 1600$ K for the {110} surface, $\approx 2600$ K for the {001} surface, and $\approx 2900$ K for the bulk, indicating that QLD fails at lower $T$ for the surfaces than for the bulk, due possibly to surface modes with a high amplitude of vibration. It is tempting to suggest that surface melting occurs at temperatures below the bulk melting temperature (3100 K). Reference 8 contains results for a wider range of oxide surfaces.

## 3.5. Defect Energies and Defect Volumes—Ba$^{2+}$ in MgO

A large Ba$^{2+}$ substituted for Mg$^{2+}$ in MgO distorts the lattice greatly. Our detailed study of the defect free energies, enthalpies, and volumes over the range 0–1500 K, based on the full minimization of all strains, has been given previously [24].

A superlattice of defects is introduced throughout the macroscopic crystal. The periodicity is then of the superlattice; the supercell contains

many atoms whose equilibrium positions are not wholly determined by symmetry but are described by a set of dimensionless internal strain coordinates $\varepsilon_k$. Defect properties, denoted by lowercase letters (e.g., $g_p$ denotes the change in Gibbs free energy at constant pressure) can then be computed *both* at constant pressure *and* at constant volume; e.g.,

$$f_v = f_v(V, T) = \{F_{dc}(V, T) - F_{pc}(V, T)\}/N_d;$$
$$g_p = g_p(P, T) = \{G_{dc}(P, T) - G_{pc}(P, T)\}/N_d \tag{5}$$

Subscripts *dc* and *pc* denote "defect crystal" and "perfect crystal," respectively, and quantities in capital letters are free energies ($F$, $G$) of the macroscopic crystal; $N_d$ is the total number of defects in the macroscopic crystal. No account therefore is taken here of the configurational entropy of randomly positional defects in the lattice; this is asymptotically correct for a single isolated defect and convergence toward properties of an isolated defect occurs as the superlattice spacing is increased.

To calculate $f_v$, the external strain is kept constant while the internal degrees of freedom are varied to give the equilibrium configuration at temperature $T$. Similarly, for $g_p$, both external and internal strains are varied to be consistent with the specified pressure. $u_v$ and $h_p$ are determined from the terms that contribute to $f_v$ and $g_p$. The volume of formation of the defect, $v_p$, follows immediately from the minimization of $F + P_{ext}V$.

Figure 3 shows $h_p(T)$ and $u_v(T)$ vs $T$, for a supercell of 216 ions containing one $Ba^{2+}$. $h_p$ is always greater than $u_v$ above $T = 0$; in the *isolated* defect limit [25] $h_p - u_v = (\beta T/\chi_T) v_p$, where $v_p$ is the defect volume. Here both $\beta$ and $v_p$ are positive. The $T$ dependence of $u_v$ is much larger than that of $h_p$ and *opposite* in sign. The results confirm the traditional assumption [25, 26] that $u_v(0)$ and $u_v(\text{static})$ are fair approximations to $h_p(T)$. $u_v(\text{static})$ is a better approximation when $T > \Theta_D$. While the high-temperature values of $u_v$ extrapolate back toward $u_v(\text{static})$, this is not true of $h_p$. Where, as here, the thermodynamic quantity of interest is determined by the relatively small difference between two large quantities ($h_p \approx 16$ eV; cf. an enthalpy of $\approx 4400$ eV for a supercell of 216 ions), the high precision of the lattice dynamics approach is particularly valuable.

## 3.6. Solid Solutions

Disorder in polar solids has been investigated theoretically largely via point defect calculations (the dilute limit) or, as in the previous section, via supercells. These methods are not readily extended to mixtures or disordered systems with a finite impurity or defect content. Instead, we have developed a configurationally averaged *lattice dynamics* approach to solid
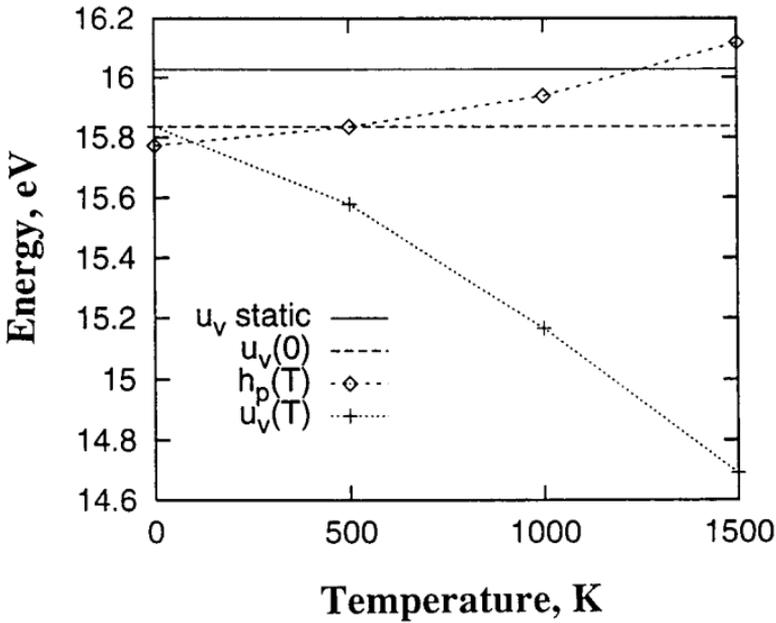
**Fig. 3.** Temperature variation of $h_p$ ($\diamond$) and $u_v$ ($+$) for a supercell of MgO containing 216 ions, with one $Mg^{2+}$ replaced by $Ba^{2+}$. $u_v(0)$ and $u_v$(static) are also shown.

solutions [27], which evaluates an appropriate thermodynamic average over a (limited) set of calculations for different configurations of cations within a supercell. If $G_k$ is the optimized free energy of configuration $k$, the enthalpy and entropy of the solid solution are approximated by

$$\langle H \rangle = \frac{\sum_k H_k \exp(-G_k/k_B T)}{\sum_k \exp(-G_k/k_B T)}, \qquad \langle S \rangle = \frac{\langle H \rangle}{T} + k_B \ln \sum_k \exp(-G_k/k_B T) \tag{6}$$

Figure 4 shows values of $\Delta H_{mix}$ for MnO/MgO obtained in this way with a unit cell of 64 atoms and 32 randomly chosen cation arrangements. The interionic potentials were taken from Ref. 28. The cell size and the number of cation arrangements are sufficient to give convergence in $\Delta H_{mix}$ to 0.1 kJ·mol$^{-1}$. There is excellent agreement (Fig. 4) between QLD and a novel Monte Carlo exchange (MCX) technique also developed by us for solid solutions [29]. The enthalpy of mixing at 1300 K is symmetric, with a maximum $\approx 5.4$ kJ·mol$^{-1}$ (50% MgO, 50% MnO). Agreement with the experimental data of Gripenberg et al. [30] is good; we do not see the asymmetry reported by Raghavan [31]. The calculated value of $\Delta H_{mix}$ varies only slightly with temperature. The failure of the mean field (MF)
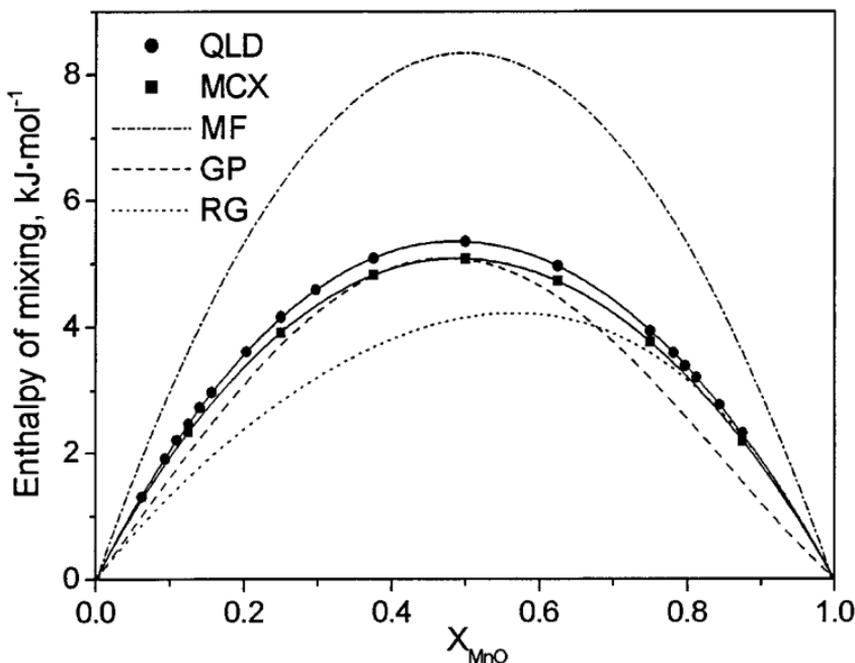
**Fig. 4.** Calculated values of $\Delta H_{mix}$ at 1000 K for MnO/MgO given by configurational lattice dynamics (QLD), exchange Monte Carlo (MCX), and mean field theory (MF). Two sets of experimental data are also shown (RG from Ref. 30, GP from Ref. 31).

approximation shows that local structural relaxation or clustering is important.

QLD is particularly useful for quantities such as entropies of mixing since free energies are obtained so readily. $\Delta S_{mix}$ includes *both* configurational *and* vibrational contributions; no assumptions are made about the ideality of the solid solution. Thus calculated entropies of mixing for CaO/MgO (for mole fractions of CaO less than 0.15) show that $\Delta S_{mix}$ is larger than the "ideal" value; as with the isolated Ba defect in MgO, the vibrational contribution is positive. This work is currently being extended to $\Delta G_{mix}$ and so to phase diagrams.

## 4. CONCLUSIONS

QLD is an economical and precise tool for not only the bulk, but also surfaces, defects, and solid solutions. New methods, such as explicit free energy minimization of a large number of configurations, can deal with high defect levels and increase considerably the contact between experiment and theory in many areas of materials and solid-state research. Future

applications include calculating ceramic and minerological data (e.g., phase diagrams), possibly at high pressures, and kinetic and mechanistic aspects of solid-state reactions. Codes for ionic solids and metals (using the embedded atom model) are available from the authors [32].

Many properties are highly sensitive to the interionic potentials. In recent years improved potentials have been obtained by fitting to *ab initio* calculations, but in the long run, with increasing computer power, it may be better to develop direct *ab initio* MD and QLD techniques.

## ACKNOWLEDGMENTS

## REFERENCES

1. M. B. Taylor, G. D. Barrera, N. L. Allan, T. H. K. Barron, and W. C. Mackrodt, *Comp. Phys. Comm.* **109**:135 (1998). (See Ref. 28 for contact details for obtaining copies of the codes.)
2. N. L. Allan, T. H. K. Barron, and J. A. O. Bruno, *J. Chem. Phys.* **105**:8300 (1996).
3. L. N. Kantorovich, *Phys. Rev. B* **51**:3520, 3535 (1995).
4. A. B. Pippard, *The Elements of Classical Thermodynamics* (Cambridge University Press, Cambridge, 1964).
5. D. C. Wallace, *Thermodynamics of Crystals* (Wiley, New York, 1972).
6. M. B. Taylor, G. D. Barrera, N. L. Allan, and T. H. K. Barron, *Phys. Rev. B* **57**:14380 (1997).
7. M. B. Taylor, N. L. Allan, J. A. O. Bruno, and G. D. Barrera, *Phys. Rev. B* **59**:353 (1999).
8. M. B. Taylor, C. E. Sims, G. D. Barrera, and N. L. Allan, *Phys. Rev. B* **59**:6742 (1999).
9. P. J. Harley, *Numerical Algorithms*, J. L. Mohamed and J. E. Walsh, eds. (Clarendon Press, Oxford, 1986), p. 239.
10. G. D. Barrera, M. B. Taylor, N. L. Allan, T. H. K. Barron, L. N. Kantorovich, and W. C. Mackrodt, *J. Chem. Phys.* **107**:4337 (1997).
11. Y. S. Touloukian, R. K. Kirby, R. E. Taylor, and T. Y. R. Lee (eds.), *Thermophysical Properties of Matter (TPRC Data Series)*, *Vol. 13* (IFI/Plenum, New York–Washington, DC, 1977).
12. T. A. Mary, J. S. O. Evans, T. Vogt, and A. W. Sleight, *Science* **272**:90 (1996).
13. J. S. O. Evans, T. A. Mary, T. Vogt, M. A. Subramanian, and A. W. Sleight, *Chem. Mater.* **8**:2809 (1996).
14. T. H. K. Barron, *Thermal Expansion of Solids*, C. Y. Ho, ed. (ASM International, Materials Park, OH, 1998), pp. 1–108.
15. A. K. A. Pryde, K. D. Hammonds, M. T. Dove, V. Heine, J. D. Gale, and M. C. Warren, *J. Phys. Condens. Matter* **8**:10973 (1996).
16. J. S. O. Evans, Z. Hu, J. D. Jorgensen, D. N. Argyriou, S. Short, and A. W. Sleight, *Science* **275**:61 (1997).

17. C. A. Swenson, *Thermal Expansion of Solids*, C. Y. Ho, ed. (ASM International, Materials Park, OH, 1998), pp. 207–224.
18. T. H. K. Barron and G. K. White, *Heat Capacity and Thermal Expansion at Low Temperatures* (Kluwer Academic/Plenum, New York, 1999).
19. J. A. O. Bruno, N. L. Allan, and T. H. K. Barron, *J. Phys. Condens. Matter* **12**:549 (2000)
20. J. A. O. Bruno, N. L. Allan, T. H. K. Barron, and A. D. Turner, *Phys. Rev. B* **58**:8416 (1998).
21. A. M. Stoneham and M. J. L. Sangster, *Phil. Mag. B* **43**:597 (1981).
22. P. W. Tasker, *Computer Simulation of Solids*, C. R. A. Catlow and W. C. Mackrodt, eds. (Springer-Verlag, Berlin, 1982), p. 288.
23. For example, D. H. Gay and A. L. Rohl, *J. Chem. Soc. Faraday Trans.* **91**:925 (1995).
24. M. B. Taylor, G. D. Barrera, N. L. Allan, T. H. K. Barron, and W. C. Mackrodt, *Faraday Discuss.* **106**:377 (1997).
25. C. R. A. Catlow, J. Corish, P. W. M. Jacobs, and A. B. Lidiard, *J. Phys. C* **14**:L125 (1981).
26. N. L. Allan, W. C. Mackrodt, and M. Leslie, *Adv. Ceram.* **23**:257 (1987).
27. J. A. Purton, J. D. Blundy, M. B. Taylor, G. D. Barrera, and N. L. Allan, *Chem. Commun.* 627 (1998).
28. G. V. Lewis and C. R. A. Catlow, *J. Phys. Sol. State Phys.* **18**:1149 (1985).
29. J. A. Purton, G. D. Barrera, N. L. Allan, and J. D. Blundy, *J. Phys. Chem. B* **102**:5202 (1998).
30. S. Raghavan, Ph.D. thesis (Indian Institute of Science, Bangalore, 1971).
31. H. Gripenberg, S. Seetharaman, and L. I. Staffansson, *Chem. Scr.* **13**:162 (1978–1979).
32. E-mail: n.l.allan@bris.ac.uk or gdb@quimica.unp.edu.ar